Supporting Information for publication

Substituent Effect on the Packing Architecture of Adamantane and Memantine Derivatives of Sulfonamide Molecular Crystals

Alexander P. Voronin[a], Tatiana V. Volkova[a], Andrey B. Ilyukhin[b], Alexey N. Proshin[c], German L. Perlovich[a,]*

[a]G.A. Krestov Institute of Solution Chemistry, Russian Academy of Sciences, 153045 Ivanovo, Russia;

[b]Institute of General and Inorganic Chemistry RAS, Leninsky Prosp. 31, 119991 Moscow, Russia;

[c]Institute of Physiologically Active Compounds, Russian Academy of Sciences, 142432, Chernogolovka, Russia;

* To whom correspondence should be addressed:

Telephone: +7-4932-533784; Fax: +7-4932-336237; E-mail glp@isc-ras.ru

Table of Contents:

Materials and Methods

S1 Synthesis and identification

S1.1 General procedure of the synthesis of the compounds studied

Synthesis of the novel sulfonamide derivatives was carried out according to Scheme S1.

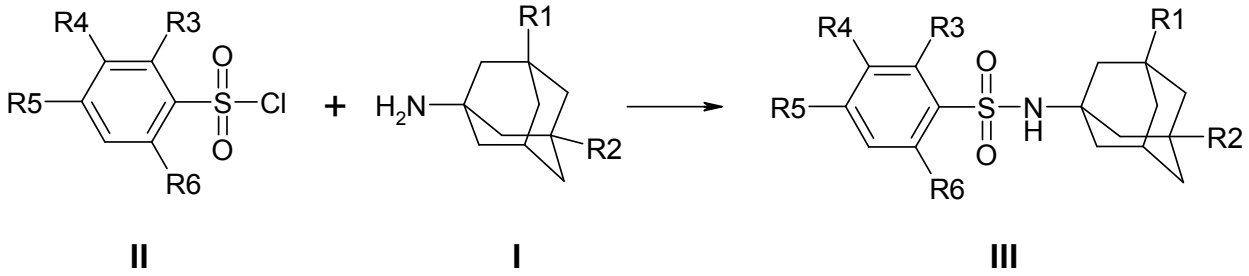

Scheme S1. Schematic diagram of synthesis of novel sulfonamides

Triethylamine (0.04 mol) was added to a stirred suspension of 1-aminoadamantane (**I**) (or Memantine, $R^1 = CH_3$) (0.01 mol) in isopropanol (30 ml) at 0°C, followed by solid sulfonyl chloride (**II**) ($R^2 = H$, $R^3 = H$, $R^4 = OMe$, $R^5 = H$ (for **15**); $R^2 = OCF_3$, $R^3 = H$, $R^4 = H$, $R^5 = H$ (for **16** and **17**); $R^2 = H$, $R^3 = H$, $R^4 = NH\text{-}C(O)\text{-}CH_3$, $R^5 = H$ (for **18** and **19**); $R^2 = H$, $R^3 = CF_3$, $R^4 = H$, $R^5 = H$ (for **20** and **21**); $R^2 = NO_2$, $R^3 = H$, $R^4 = H$, $R^5 = H$ (for **22**); $R^2 = CH_3$, $R^3 = H$, $R^4 = CH_3$, $R^5 = CH_3$ (for **23** and **24**)) (0.01 mol) over a period of 30 minutes. The reaction mixture was heated at 60°C for 2 hours, after which HPLC showed that there was no starting material left. The resulting suspension was cooled to room temperature and the precipitate of triethylamine hydrochloride was removed by filtration. The filtrate was evaporated to dryness to afford a colorless oil which was dissolved in ethyl acetate (50 ml), washed with 0.5N HC1 (50 ml), water (50 ml) and dried over $MgSO_4$. The solvent was evaporated by a rotary evaporator to afford sulfonamide as a white crystalline solid. Yields: 80-90%.

The compounds were carefully purified by re-crystallising from water-ethanol solution. The precipitate was filtered and dried at room temperature under vacuum until the mass of compounds remained constant. The outlined procedure was repeated several times and the product checked by NMR after each re-crystallization step until the proton NMR signal correspondence to the purity of the compound was over 98-99 %.

S1.2 NMR Experiments

^{1}H NMR spectra were recorded on Bruker CXP-200 instrument (Germany) with $CDCl_3$ used as a solvent.

N-(3,5-Dimethyl-adamantan-1-yl)-4-methoxy-benzenesulfonamide (**15**)

^{1}H NMR (200 MHz, $CDCl_3$), δ, ppm: 0.79 (s, 6H, $2CH_3$), 1.07 (s, 2H, AdH), 1.23 (m, 4H, AdH), 1.44 (m, 4H, AdH), 1.60 (d, J = 2.44, 1H, AdH), 2.06 (m, 1H, AdH), 3.88 (s, 3H, OCH_3), 5.21 (s, 1H, NH), 6.95 (d, J = 8.53 Hz, 2H, ArH), 7.82 (d, J = 8.53 Hz, 2H, ArH). Mp 138.9°C. Anal. ($C_{19}H_{27}NO_3S$) C, H, N, S.

N-Adamantan-1-yl-2-trifluoromethoxy-benzenesulfonamide (**16**)

^{1}H NMR (200 MHz, $CDCl_3$), δ, ppm: 1.68 (m, 6H, AdH), 1.78 (d, J = 2.44 Hz, 6H, AdH), 2.00 (br. s., 3H, AdH), 4.63 (s, 1H, NH), 7.39 (m, 2H, ArH), 7.81 (td, J = 7.92, 1.83 Hz, 1H, ArH), 8.06 (dd, J = 7.92, 1.83 Hz, 1H, ArH). Mp 131.9°C. Anal. ($C_{17}H_{20}F_3NO_3S$) C, H, N, S.

N-(3,5-Dimethyl-adamantan-1-yl)-2-trifluoromethoxy-benzenesulfonamide (**17**)

^{1}H NMR (200 MHz, $CDCl_3$), δ, ppm: 0.77 (s, 6H, $2CH_3$), 1.06 (s, 2H, AdH), 1.23 (m, 4H, AdH), 1.42 (m, 4H, AdH), 1.59 (m, 2H, AdH), 2.05 (m, 1H, AdH), 4.65 (s, 1H, NH), 7.40 (m, 2H, ArH), 7.61 (d, *J* = 7.62 Hz, 1H, ArH), 8.04 (d, *J* = 7.92 Hz, 1H, ArH). Mp 126.3°C. Anal. ($C_{19}H_{24}F_3NO_3S$) C, H, N, S.

N-[4-(Adamantan-1-ylsulfamoyl)-phenyl]-acetamide (**18**)

^{1}H NMR (200 MHz, $CDCl_3$), δ, ppm: 1.56 (m, 6H, AdH), 1.78 (d, *J* = 2.44 Hz, 6H, AdH), 2.00 (br. s., 3H, AdH), 2.20 (s, 3H, CH_3), 4.92 (s, 1H, NH), 7.64 (d, *J* = 7.92 Hz, 2H, ArH), 7.78 (d, *J* = 7.92 Hz, 2H, ArH), 8.26 (m, 1H, ArNH). Mp 217.4°C. Anal. ($C_{18}H_{24}N_2O_3S$) C, H, N, S.

N-[4-(3,5-Dimethyl-adamantan-1-ylsulfamoyl)-phenyl]-acetamide (**19**)

^{1}H NMR (200 MHz, $CDCl_3$), δ, ppm: 0.82 (s, 6H, $2CH_3$), 1.10 (s, 2H, AdH), 1.27 (m, 4H, AdH), 1.47 (m, 4H, AdH), 1.64 (c, 2H, AdH), 2.08 (m, 1H, AdH), 2.26 (s, 3H, CH_3), 4.51 (s, 1H, NH), 7.52 (s, 1H, ArNH), 7.62 (dd, *J* = 9.14, 2.44 Hz, 2H, ArH), 7.81 (dd, *J* = 9.14, 2.44 Hz, ArH). Mp 232.0°C. Anal. ($C_{20}H_{28}N_2O_3S$) C, H, N, S.

N-Adamantan-1-yl-3-trifluoromethyl-benzenesulfonamide (**20**)

^{1}H NMR (200 MHz, $CDCl_3$), δ, ppm: 1.59 (m, 6H, AdH), 1.81 (d, *J* = 2.44 Hz, 6H, AdH), 2.03 (br. s., 3H, AdH), 4.69 (s, 1H, NH), 7.65 (t, *J* = 7.92 Hz, 1H, ArH), 7.81 (d, *J* = 7.92 Hz, 1H, ArH), 8.11 (d, *J* = 7.92 Hz, 1H, ArH), 8.17 (c, 1H, ArH). Mp 111.7°C. Anal. ($C_{17}H_{20}F_3NO_2S$) C, H, N, S.

N-(3,5-Dimethyl-adamantan-1-yl)-3-trifluoromethyl-benzenesulfonamide (**21**)

^{1}H NMR (200 MHz, $CDCl_3$), δ, ppm: 0.82 (s, 6H, $2CH_3$), 1.11 (s, 2H, AdH), 1.28 (m, 4H, AdH), 1.54 (m, 4H, AdH), 1.71 (m, 2H, AdH), 2.11 (m, 1H, AdH), 5.21 (s, 1H, NH), 7.74 (m, 2H, ArH), 7.86 (m, 1H, ArH), 8.21 (m, 1H, ArH). Mp 132.3°C. Anal. ($C_{19}H_{24}F_3NO_2S$) C, H, N, S.

N-(3,5-Dimethyl-adamantan-1-yl)-2-nitro-benzenesulfonamide (**22**)

^{1}H NMR (200 MHz, $CDCl_3$), δ, ppm: 0.82 (s, 6H, $2CH_3$), 1.11 (s, 2H, AdH), 1.28 (m, 4H, AdH), 1.53 (m, 4H, AdH), 1.71 (d, *J* = 2.44, 2H, AdH), 2.11 (m, 1H, AdH), 5.21 (s, 1H, NH), 7.73 (m, 2H, ArH), 7.86 (m, 1H, ArH), 8.20 (m, 1H, ArH). Mp 193.1°C. Anal. ($C_{18}H_{24}N_2O_4S$) C, H, N, S.

N-Adamantan-1-yl-2,4,6-trimethyl-benzenesulfonamide (**23**)

^{1}H NMR (200 MHz, $CDCl_3$), δ, ppm: 1.57 (m, 6H, AdH), 1.81 (m, 6H, AdH), 1.98 (br. s., 3H, AdH), 2.28 (s, 3H, $ArCH_3$), 2.64 (s, 6H, $2ArCH_3$), 4.40 (s, 1H, NH), 6.93 (c, 2H, ArH). Mp 182.1°C. Anal. ($C_{19}H_{27}NO_2S$) C, H, N, S.

N-(3,5-Dimethyl-adamantan-1-yl)-2,4,6-trimethyl-benzenesulfonamide (**24**)

^{1}H NMR (200 MHz, $CDCl_3$), δ, ppm: 0.78 (s, 6H, $2CH_3$), 1.07 (s, 2H, AdH), 1.23 (m, 4H, AdH), 1.43 (m, 4H, AdH), 1.58 (m, 2H, AdH), 2.05 (m, 1H, AdH), 2.28 (s, 3H, $ArCH_3$), 2.66 (s, 6H, $2ArCH_3$), 4.42 (s, 1H, NH), 6.93 (c, 2H, ArH). Mp 192.1°C. Anal. ($C_{21}H_{31}NO_2S$) C, H, N, S

S2 Single crystals preparation

Single crystals of the compounds were grown from 96% ethanol by slow evaporation. A powder sample of the substance was fully dissolved at room temperature to yield a clear solution. The solution was filtered through a 0.22 μm PTFE syringe filter into a glass vial, then the vial was sealed by Parafilm® with few small holes pierced and the solvent was allowed to evaporate at room temperature for 3-5 days. For compound **18**, crystallisation from 96% ethanol resulted in **18**·$2H_2O$ (crystallographic data are given in Table S2). Single crystals of anhydrous **18** were obtained from HPLC grade methanol.

S3 Analytical methods

S3.1 X-ray diffraction experiments

Experimental data from single crystals **15-22, 24, 18·2H$_2$O** were obtained on a Bruker SMART APEX2 diffractometer [1] (Table 1). Absorption for **15-22, 24, 18·2H$_2$O** was taken into account by a semiempirical method based on equivalents using SADABS software [2]. Experimental data from single crystal **23** was obtained on a Enraf Nonius CAD-4 diffractometer [3] (Table 1). The structures were determined using a combination of the direct method and Fourier syntheses. All the calculations were carried out using SHELXS and SHELXL software [4].

During the space group determination of structure **19**, it was found out that the reflections of type h+k=2n+1 are systematically absent, and **B** type alerts occur during the check of refinement results:

```
PLAT110_ALERT_2_B ADDSYM Detects Potential Lattice Translation
... ? Check
PLAT112_ALERT_2_B ADDSYM Detects New (Pseudo) Symm. Elem. I 100
%Fit
PLAT113_ALERT_2_B ADDSYM Suggests Possible Pseudo/New Space
Group I2/c Check
Note: (Pseudo) Lattice Translation Implemented
```

Structure refinement in the centrosymmetric group leads to disorder that can be removed by selecting the primitive cell. Diffraction experiments conducted at 150, 298 and 350 K for a single sample along with data collected for two other single crystal samples have demonstrated that a phase transition occurs in **19** in a wide temperature range. Table S1 summarises the statistics on the intensity of reflections of type h+k=2n+1 with integration performed in the primitive unit cell:

Table S1. Intensities of reflections of type h+k=2n+1 in crystal **19** recorded at different temperatures

Temperature	150 K		298 K		350 K	
Lattice exceptions	P	All	P	All	P	All
N (total)	25513	25412	28300	28276	14797	14707
N (int > 3σ)	6936	18418	6	13295	2	9289
Mean intensity	0.7	14.6	0.1	15.1	0.1	10.1
Mean int/σ	2.6	9.7	0.3	8.8	0.4	10.7

S3.2 Differential scanning calorimetry

Differential scanning calorimetry (DSC*)* was carried out using a Perkin-Elmer Pyris 1 DSC differential scanning calorimeter (Perkin Elmer Analytical Instruments, Norwalk, Connecticut, USA) with Pyris software for Windows NT. DSC runs were performed in a flow of dry nitrogen (20 ml·min^{-1}) using standard aluminum sample pans and at a heating rate of 10 K·min^{-1}. The accuracy of weight measurements was ± 0.005 mg. The DSC was calibrated with internal standard indium and zinc samples from Perkin-Elmer (P/N 0319-0033). The value determined for the fusion enthalpy of indium corresponded to 28.48 J·g^{-1} (reference value 28.45 J·g^{-1}). The melting point of indium was 156.5±0.1° C (n=10), of zinc – 419.7±0.1° C (n=5).

S4 Calculation procedure

S4.1 Free molecular volume calculation

The free molecular volume in the crystal lattice was estimated on the basis of the X-ray diffraction data and van-der-Waals molecular volume (V^{vdw}), calculated by GEPOL: [7]

$$V^{free} = (V_{cell} - Z \cdot V^{vdw}) / Z \quad \text{(S1)}$$

where V_{cell} is the volume of the unit cell, Z is the number of molecules in the unit cell.

S4.2 XPac analysis

The quantitative analysis of packing similarity was performed using XPac v. 2.0.2. [8] This method allows finding the isostructural supramolecular constructs within the pairs of crystals by comparing the relative position and orientation of identical molecular graphs named 'common sets of points' in clusters which imitate the crystal environment of a molecule. The measure of packing similarity is the dissimilarity index X, which shows the difference in angles δ_a and interplanar angles δ_p, and stretch parameter D, which indicates the difference in distances between the nearest identical fragments. Lattice parameters and positions of all heavy atoms used in the calculation were taken from the X-Ray experiment. A cluster of 15 molecules with intermolecular atom-atom distance shorter than sum of van-der-Waals radii of contact atoms +1.5 Å was considered for each crystal. Medium-level threshold values for parameters δ_a and δ_p were used, which equals 10° and 14°, respectively.

S4.3 Hydrogen bond energy calculation

The hydrogen bonding energy was calculated with the help of Mayo et al.[9] force field:

$$E_{HB} = D_{HB} \cdot [5(R_{hb}/R_{DA})^{12} - 6(R_{hb}/R_{DA})^{10}] \cdot \cos^4(\theta_{DHA}) \quad \text{(S2)}$$

where D_{HB} = 39.7 kJ·mol^{-1} is a depth of potential well of pair potential at creation of hydrogen bond of H_2O dimer; R_{hb}=2.75 Å; R_{DA}, θ_{DHA} are the distance and angle between donor and acceptor atoms.

S4.4 Solid-state DFT calculations followed by QTAIMC analysis of periodic electron density

Density functional theory computations with periodic boundary conditions (solid-state DFT) were performed in the Crystal14 software package [10] using meta-GGA B3LYP functional in localized 6-31G(d,p) basis set. The B3LYP/6-31G(d,p) approximation was proven to provide reliable and consistent results in studying the intermolecular interactions in crystals.[11] Since dispersive interactions are supposed to contribute significantly into the stability of the crystal lattice, the D2 empirical correction by Grimme et al. was used in periodic wavefunction calculations.[12] The unit cell parameters and positions of heavy atoms determined with high accuracy from low-temperature X-Ray diffraction experiment were fixed, while the coordinates of hydrogen atoms were optimized for all structures. Bader analysis [13] of periodic electron density, or QTAIMC [14] was performed in TOPOND14, [15] and search for (3;-1) critical points was conducted between the pairs of atoms within the 5Å radius around each symmetry-inequivalent atom in unit cell. The following electron-density features at the bond critical point were computed for every non-covalent interaction: (i) the values of the electron density, ρ_b, (ii) the Laplacian of the electron density, $\nabla^2\rho_b$, and (iii) the positively defined local electronic kinetic energy density, G_b. The threshold on ρ_b for considered interactions was set as 0.003 a.u. since weaker interactions are too small for determination by existing experimental and computational methods.[46] The energy of the particular single non-covalent interaction E_{int} was estimated using the equation proposed by Mata et al.: [16]

$$E_{int}\ (\text{kJ·mol}^{-1}) = 1147 \cdot G_b\ (\text{a.u.}) \quad \text{(S3)}$$

Equation (7) yields reasonable E_{int} values for molecular crystals with different types of intermolecular interactions: H-bonds, C−H···O, H···H and π-stacking contacts, etc. [49]

Total cohesion energy[50] was calculated as sum of energies of all intermolecular interactions in the asymmetric unit as described elsewhere:

$$E_{latt} = \sum_i \sum_{j<i} E_{\text{int},j,i} \quad \text{(S4)}$$

where $E_{\mathrm{int},j,i}$ is the energy of a particular noncovalent interaction. Indices *j* and *i* denote the atoms belonging to different molecules. The presented approach provides reasonable values for single-component [17] and two-component [18,19] molecular crystals.

S4.5 Hirshfeld surface analysis

The analysis of Hirshfeld surfaces [20] of molecules within the crystal was performed in *CrystalExplorer* v.3.1. [21] The surface resolution was set to 'Very High'. The distances from the Hirshfeld surface to the nearest nucleus outside and inside the surface (d_e and d_i, respectively) were plotted into a 2D fingerprint map. The contributions from interactions between atoms of different types into the surface were calculated basing on the normalized distance of intermolecular contact d_{norm} [22] between different pairs of nuclei calculated as:

$$d_{norm} = \frac{d_i - r_i^{vdW}}{r_i^{vdW}} + \frac{d_e - r_e^{vdW}}{r_e^{vdW}} \qquad \text{(S5)}$$

where r_i^{vdW} and r_i^{vdW} are the van-der-Waals radii of contact atoms inside and outside the Hirshfeld surface.

References:

1 Bruker (2007). APEX2 and SAINT. Bruker AXS Inc., Madison, Wisconsin, USA.
2 G. M. Sheldrick, SADABS. University of Göttingen, Germany, 1997.
3 Oxford Diffraction (2009). *CrysAlis CCD* and *CrysAlis RED* Oxford Diffraction Ltd, Yarnton, England.
4 G. M. Sheldrick. Crystal structure refinement with SHELXL. *Acta Cryst.*, 2015, C**71**, 3-8.
5 J. L. Pascual-Ahuir and E. Silla, *J. Comput. Chem.,* 1990, **11**, 1047-1060.
6 T. Gelbrich, D. S. Hughes, M. B. Hursthouse and T. L. Threlfall, *CrystEngComm,* 2008, **10**, 1328-1334.
7 S. L. Mayo, B. D. Olafson and W. A. Goddard III, *J Phys. Chem.,* 1990, **94**, 8897-8909.
8 R. Dovesi, R. Orlando, A. Erba, C. M. Zicovich-Wilson, B. Civalleri, S. Casassa, L. Maschio, M. Ferrabone, M. De La Pierre, P. D'Arco, Y. Noël, M. Causà, M. Rérat and B. Kirtman, *Int. J. Quantum Chem.,* 2014, **114**, 1287-1317.
9 S. A. Katsyuba, M. V. Vener, E. E. Zvereva, Z. Fei, R. Scopelliti, J. G. Brandenburg, S. Siankevich and P. J. Dyson, *J. Phys. Chem. Lett.,* 2015, **6**, 4431-4436.
10 S. J. Grimme, *J. Comput. Chem.,* 2006, **27**, 1787–1799.
11 R. F. W. Bader, Atoms in Molecules - A Quantum Theory. Oxford University Press: Oxford, 1990.
12 V. G. Tsirelson and R. P. Ozerov, Electron Density and Bonding in Crystals. Bristol, England / Philadelphia, USA: Institute of Physics Publishing. 1996.
13 C. Gatti and S. Casassa, TOPOND14 User's Manual, CNR-ISTM Milano, Milano, 2014.
14 I. Mata, I. Alkorta, E. Espinosa and E. Molins, *Chem. Phys. Lett.,* 2011, **507**, 185-189.
15 M. V. Vener, E. O. Levina, O. A. Koloskov, A. A. Rykounov, A. P. Voronin and V. G. Tsirelson, *Cryst. Growth Des.,* 2014, **14**, 4997-5003.
16 P. M. Dominiak, E. Espinosa and J. Ángyán, In *Modern Charge Density Analysis*; Editors: C. Gatti and P. Macchi, Springer, Heidelberg, 2012, 387-433.
17 Y. A. Abramov, A. Volkov, G. Wu and P. Coppens, *J. Phys. Chem. B,* 2000, **104**, 2183-2188.
18 A. N. Manin, A. P. Voronin, A. V. Shishkina, M. V. Vener, A. V. Churakov and G. L. Perlovich, *J. Phys. Chem. B,* 2015, **119**, 10466-10477.
19 A. O. Surov, A. V. Churakov and G. L. Perlovich, *Cryst. Growth & Des.,* 2016, **16**, 6556-6567.

20 M. A. Spackman and D. Jayatilaka, *CrystEngComm,* 2009, **11**, 19-32.
21 S. K. Wolff, D. J. Grimwood, J. J. McKinnon, M. J. Turner, D. Jayatilaka and M. A. Spackman, CrystalExplorer, Version 3.1. University of Western Australia, Crawley, Australia, 2012.
22 J. J. McKinnon, D. Jayatilaka and M. A. Spackman, *Chem. Commun.,* 2007, 3814-3816.

Table S2. Crystal data and structure refinement for **15-24**.

Identification code	**15**	**16**	**17**	**18**
CCDC number	1962767	1962768	1962769	1962770
Empirical formula	$C_{19}H_{27}NO_3S$	$C_{17}H_{20}F_3NO_3S$	$C_{19}H_{24}F_3NO_3S$	$C_{18}H_{24}N_2O_3S$
Formula weight	349.47	375.40	403.45	348.45
Temperature, K	120(2)	150(2)	150(2)	150(2)
Wavelength, Å	0.71073	0.71073	0.71073	0.71073
Crystal system	Monoclinic	Monoclinic	Monoclinic	Triclinic
Space group	$P2_1/c$	$P2_1/n$	$P2_1/n$	P-1
a, Å	10.5390(3)	11.0788(5)	10.5361(6)	12.0138(6)
b, Å	15.4431(4)	12.2658(6)	11.2474(6)	12.6480(6)
c, Å	11.3497(3)	12.9608(6)	16.3452(10)	13.5487(7)
α, °	90	90	90	107.167(2)
β, °	105.2140(10)	108.4380(10)	100.077(2)	111.066(2)
γ, °	90	90	90	97.215(2)
Volume, $Å^3$	1782.48(8)	1670.84(14)	1907.09(19)	1772.49(16)
Z	4	4	4	4
D (calc), Mg/m^3	1.302	1.492	1.405	1.306
μ, mm^{-1}	0.198	0.242	0.218	0.201
F(000)	752	784	848	744
Crystal size, mm	0.38 x 0.36 x 0.2	0.3 x 0.26 x 0.2	0.42 x 0.3 x 0.24	0.28 x 0.2 x 0.12
θ range, °	2.280, 31.497	2.114, 31.520	2.142, 32.565	2.209, 27.906
Index ranges	-15<=h<=14	-16<=h<=16	-13<=h<=15	-15<=h<=15
	-21<=k<=22	-18<=k<=17	-17<=k<=14	-16<=k<=16
	-15<=l<=13	-18<=l<=18	-23<=l<=24	-17<=l<=17
Reflections collected	21884	24560	20427	21923
Independent reflections, Rint	5620, 0.0310	5546, 0.0419	6606, 0.0324	8422, 0.0402
Completeness to θ = 25.242°	100.0 %	100.0 %	100.0 %	99.9 %
Absorption correction	Semi-empirical from equivalents	Semi-empirical from equivalents	Semi-empirical from equivalents	Semi-empirical from equivalents
Max,. min. transmission	0.6481, 0.545	0.7462, 0.6711	0.7464, 0.649	0.7456, 0.6569
Refinement method	Full-matrix least-squares on F^2	Full-matrix least-squares on F^2	Full-matrix least-squares on F^2	Full-matrix least-squares on F^2
Data / restraints / parameters	5620 / 0 / 325	5546 / 0 / 306	6606 / 0 / 340	8422 / 0 / 565
Goodness-of-fit	1.012	0.993	1.080	1.005
R1, wR2 [I>2sigma(I)]	0.0368, 0.0965	0.0449, 0.1215	0.0428, 0.1216	0.0466, 0.1128
R1, wR2 (all data)	0.0450, 0.1025	0.0589, 0.1321	0.0581, 0.1326	0.0750, 0.1264
Largest diff. peak and hole, $e.Å^{-3}$	0.621, -0.424	0.631, -0.289	0.531, -0.397	0.415, -0.431

Identification code	**19_150K**	**19_298K**	**19_350K**	**20**	**21**
CCDC number	1962771	1962772	1962773	1962774	1962775
Empirical formula	$C_{20}H_{28}N_2O_3S$	$C_{20}H_{28}N_2O_3S$	$C_{20}H_{28}N_2O_3S$	$C_{17}H_{20}F_3NO_2S$	$C_{19}H_{24}F_3NO_2S$
Formula weight	376.50	376.50	376.50	359.40	387.45
Temperature, K	150(2)	298(2)	350(2)	120(2)	120(2)
Wavelength, Å	0.71073	0.71073	0.71073	0.71073	0.71073
Crystal system	Monoclinic	Monoclinic	Monoclinic	Triclinic	Monoclinic
Space group	$P2_1/c$	C2/c	C2/c	P-1	$P2_1/n$
a, Å	18.8607(8)	19.5823(13)	19.645(4)	11.0703(5)	9.4774(4)
b, Å	15.5920(7)	15.6900(10)	15.735(3)	12.2683(5)	12.9160(6)
c, Å	14.1742(6)	14.2997(10)	14.349(3)	13.2315(6)	15.3582(7)
α, °	90	90	90	107.558(2)	90
β, °	109.2060(10)	114.189(2)	114.347(7)	90.903(2)	99.8470(10)
γ, °	90	90	90	102.794(2)	90
Volume, $Å^3$	3936.3(3)	4007.8(5)	4041.1(15)	1664.16(13)	1852.30(14)
Z	8	8	8	4	4
D (calc), Mg/m^3	1.271	1.248	1.238	1.434	1.389
μ, mm^{-1}	0.186	0.183	0.181	0.235	0.217
F(000)	1616	1616	1616	752	816
Crystal size, mm	0.4 x 0.3 x 0.26	0.4 x 0.3 x 0.26	0.4 x 0.3 x 0.26	0.36 x 0.36 x 0.06	0.34 x 0.28 x 0.18
θ range, °	2.045, 28.303	2.280, 30.049	2.276, 27.112	2.278, 29.599	2.073, 31.505
Index ranges	-25<=h<=24	-27<=h<=27	-25<=h<=17	-15<=h<=15	-13<=h<=13
	-20<=k<=20	-21<=k<=22	-19<=k<=20	-17<=k<=15	-18<=k<=18
	-18<=l<=18	-20<=l<=20	-17<=l<=18	-18<=l<=17	-21<=l<=22
Reflections collected	49779	27687	14383	21801	26169
Independent reflections, Rint	9748, 0.0472	5869, 0.0402	4409, 0.0288	8546, 0.0419	5917, 0.0325
Completeness to θ = 25.242°	100.0 %	99.9 %	99.9 %	99.9 %	100.0 %
Absorption correction	Semi-empirical from equivalents	Semi-empirical from equivalents	Semi-empirical from equivalents	Semi-empirical from equivalents	Semi-empirical from equivalents
Max,. min. transmission	0.7457, 0.6509	0.746, 0.6653	0.7455, 0.6611	0.7459, 0.6159	0.7462, 0.6661
Refinement method	Full-matrix least-squares on F^2	Full-matrix least-squares on F^2	Full-matrix least-squares on F^2	Full-matrix least-squares on F^2	Full-matrix least-squares on F^2
Data / restraints / parameters	9748 / 0 / 475	5869 / 0 / 235	4409 / 0 / 235	8546 / 54 / 481	5917 / 0 / 331
Goodness-of-fit	1.000	1.135	1.122	1.014	1.045
R1, wR2 [I>2sigma(I)]	0.0459, 0.1276	0.0501, 0.1439	0.0533, 0.1496	0.0499, 0.1146	0.0367, 0.1086
R1, wR2 (all data)	0.0771, 0.1505	0.0745, 0.1607	0.0767, 0.1646	0.0822, 0.1287	0.0455, 0.1157
Largest diff. peak and hole, $e.Å^{-3}$	0.642, -0.684	0.456, -0.476	0.345, -0.363	0.622, -0.549	0.527, -0.340

Identification code	**22**	**23**	**24**	**18·2H_2O**
CCDC number	1962776	1962777	1962778	1962779
Empirical formula	$C_{18}H_{24}N_2O_4S$	$C_{19}H_{27}NO_2S$	$C_{21}H_{31}NO_2S$	$C_{18}H_{28}N_2O_5S$
Formula weight	364.45	333.47	361.53	384.48
Temperature, K	120(2)	296(2)	120(2)	120(2)
Wavelength, Å	0.71073	1.54184	0.71073	0.71073
Crystal system	Monoclinic	Triclinic	Triclinic	Monoclinic
Space group	$P2_1/c$	P-1	P-1	Pn
a, Å	14.9094(6)	6.6214(14)	10.5236(3)	13.3372(6)
b, Å	12.1019(5)	10.2453(17)	13.9711(4)	6.7727(3)
c, Å	10.5363(5)	13.391(2)	14.1761(4)	21.8857(10)
α, °	90	91.638(14)	78.4410(10)	90
β, °	107.7580(10)	96.140(17)	85.2520(10)	101.262(2)
γ, °	90	100.447(16)	73.4320(10)	90
Volume, $Å^3$	1810.51(14)	887.2(3)	1956.48(10)	1938.84(15)
Z	4	2	4	4
D (calc), Mg/m^3	1.337	1.248	1.227	1.317
μ, mm^{-1}	0.204	1.686	0.179	0.198
F(000)	776	360	784	824
Crystal size, mm	0.32 x 0.24 x 0.2	0.28 x 0.2 x 0.18	0.4 x 0.28 x 0.24	0.28 x 0.16 x 0.14
θ range, °	2.211, 31.497	5.381, 70.045	2.181, 31.019	2.966, 30.525
Index ranges	-21<=h<=21	-8<=h<=8	-15<=h<=15	-18<=h<=18
	-17<=k<=17	-12<=k<=12	-20<=k<=19	-9<=k<=9
	-15<=l<=15	-16<=l<=16	-20<=l<=20	-31<=l<=31
Reflections collected	21690	6541	28355	26492
Independent reflections, R_{int}	5733, 0.0345	3366, 0.0358	12002, 0.0363	11607, 0.0420
Completeness to θ = 25.242°	100.0 %	99.9 %	99.9 %	99.9 %
Absorption correction	Semi-empirical from equivalents	Semi-empirical from equivalents	Semi-empirical from equivalents	Semi-empirical from equivalents
Max,. min. transmission	0.6481, 0.553		0.7462, 0.6387	0.7461, 0.6317
Refinement method	Full-matrix least-squares on F^2	Full-matrix least-squares on F^2	Full-matrix least-squares on F^2	Full-matrix least-squares on F^2
Data / restraints / parameters	5733 / 0 / 322	3366 / 0 / 216	12002 / 0 / 699	11607 / 2 / 519
Goodness-of-fit	1.040	0.983	1.016	0.986
R1, wR2 [I>2sigma(I)]	0.0372, 0.0986	0.0422, 0.1183	0.0453, 0.1152	0.0476, 0.1037
R1, wR2 (all data)	0.0466, 0.1052	0.0620, 0.1350	0.0652, 0.1265	0.0659, 0.1121
Absolute structure parameter				0.12(4)
Largest diff. peak and hole, $e.Å^{-3}$	0.545, -0.350	0.311, -0.288	0.497, -0.344	0.406, -0.289

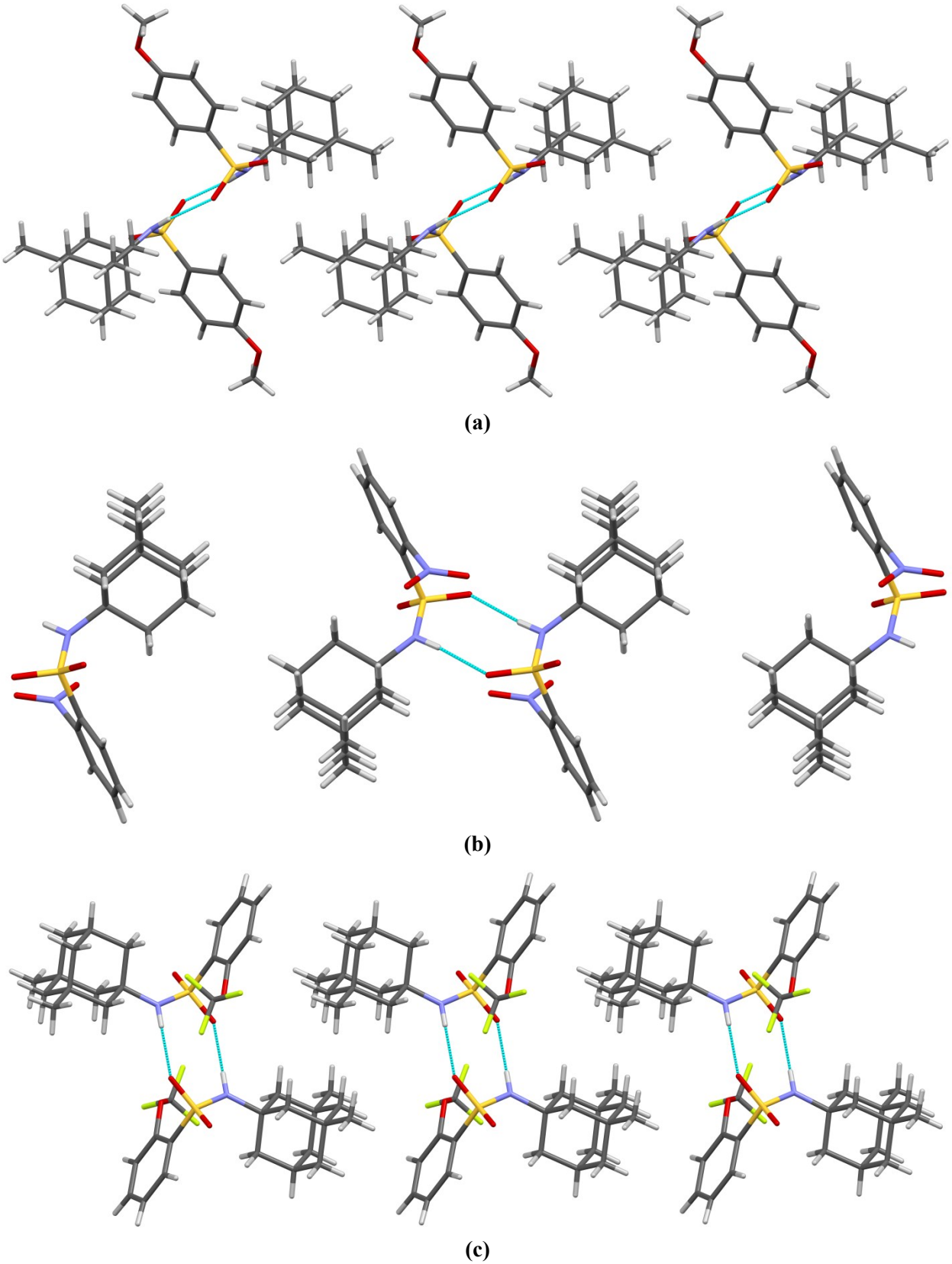

Fig. S1 (a) Part of the crystal lattice of compound **15** showing diagonal packing of hydrogen-bonded dimers along the *a* axis (supramolecular motif SC_{13}) (b) Part of the crystal lattice of compound **22** with adamantane dimer packing of hydrogen-bonded motifs (supramolecular motif SC_{14}) (c) Part of the crystal lattice of compound **17** showing phenyl-to-adamantane packing of hydrogen-bonded dimers (supramolecular motif SC_{15})

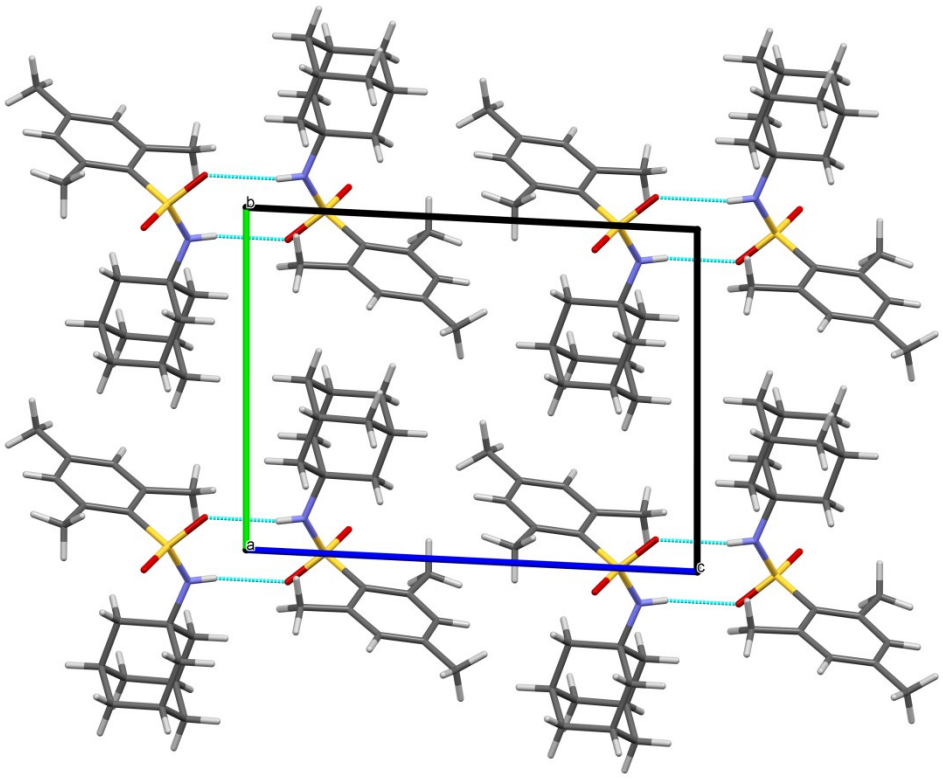

Fig. S2 Molecular packing in crystal **23** showing the two-dimensional SC_{21} supramolecular construct

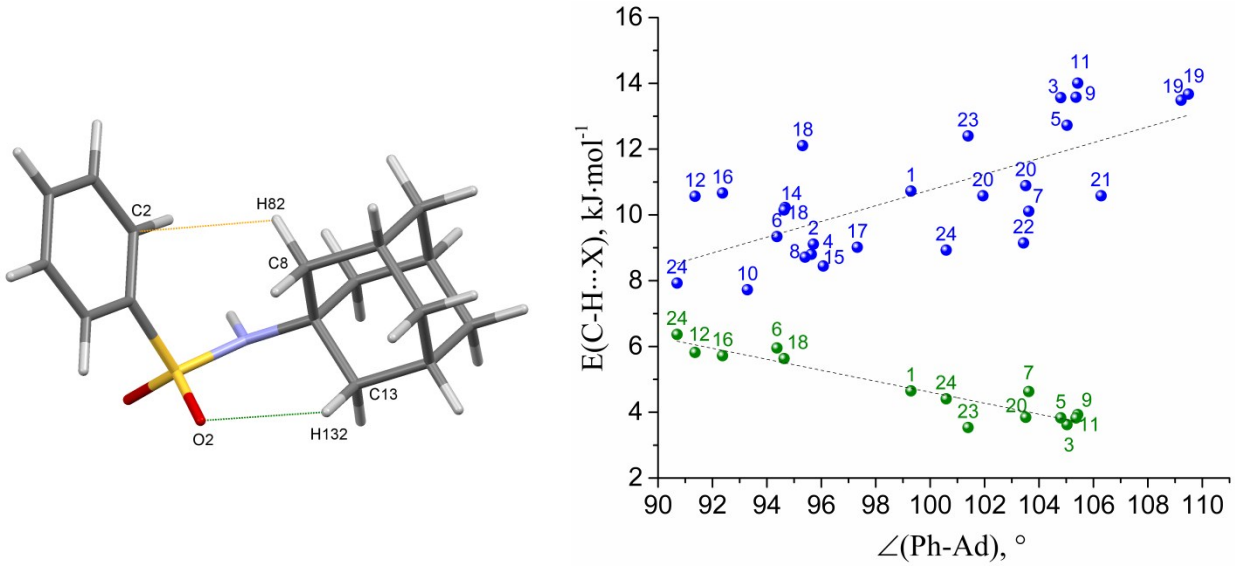

(a) **(b)**

Fig. S3 (a) Intramolecular C-H···O (green) and C-H···π (orange) contacts in considered crystals detected by QTAIMC (exemplified by compound **1**). (b) Energies of intramolecular C-H···O and C-H···π contacts in the considered crystals plotted against the dihedral angle between phenyl and adamantane fragments.

Table S3. Contributions of different types of stabilizing non-covalent interactions into the lattice energy* of crystals under study estimated by eqs. (S3) and (S4).

Compound	**15**	**16**	**17**	**18**	**19**	**20**	**21**	**22**	**23**	**24**
E_{latt}	141.6	113.1	111.9	139.5	144.4	116.7	103.5	144.9	96.8	114.9
ΣE(HB)	0.0	25.8 *19.4%*	21.3 *16.6%*	24.9 *20.0%*	20.1 *15.4%*	20.1 *14.8%*	14.3 *10.0%*	20.1 *14.3%*	20.7 *13.6%*	23.8 *16.8%*
ΣE(C-H···O)	39.6 *36.5%*	40.2 *30.2%*	12.8 *9.9%*	34.3 *27.6%*	16.8 *12.9%*	33.9 *24.9%*	38.3 *26.8%*	30.1 *21.4%*	42.9 *28.1%*	56.4 *39.8%*
ΣE(C-H···N)	2.3 *2.1%*	0.0	5.5 *4.2%*	0.0	5.5 *4.2%*	0.0	5.4 *3.8%*	0.0	5.2 *3.4%*	0.0
ΣE(C-H···C)	17.8 *16.4%*	12.8 *9.6%*	5.5 *4.2%*	6.5 *5.3%*	5.7 *4.4%*	6.8 *5.0%*	6.9 *4.8%*	5.0 *3.6%*	10.4 *6.8%*	6.7 *4.7%*
ΣE(H···H)	45.4 *41.9%*	54.2 *40.8%*	61.7 *48.0%*	42.7 *34.3%*	55.8 *42.8%*	45.5 *33.4%*	32.1 *22.5%*	36.3 *25.9%*	54.5 *35.8%*	43.5 *30.7%*
ΣE(X···X)**	3.4 *3.1%*	0.0	7.8 *6.1%*	2.5 *2.0%*	8.2 *6.3%*	5.7 *4.2%*	2.7 *1.9%*	6.1 *4.4%*	18.7 *12.3%*	11.4 *8.0%*
ΣE(C-H···Hal)	-	-	11.4 *8.9%*	11.0 *8.9%*	12.7 *9.7%*	16.8 *12.3%*	28.6 *20.0%*	36.7 *26.2%*	-	-
ΣE(X···Hal)**	-	-	2.7 *2.1%*	2.5 *2.0%*	5.6 *4.3%*	7.5 *5.5%*	14.6 *10.2%*	5.9 *4.2%*	-	-

*All energies are given in kJ·mol^{-1} and % of E_{latt} values;
**X = C, N, O.

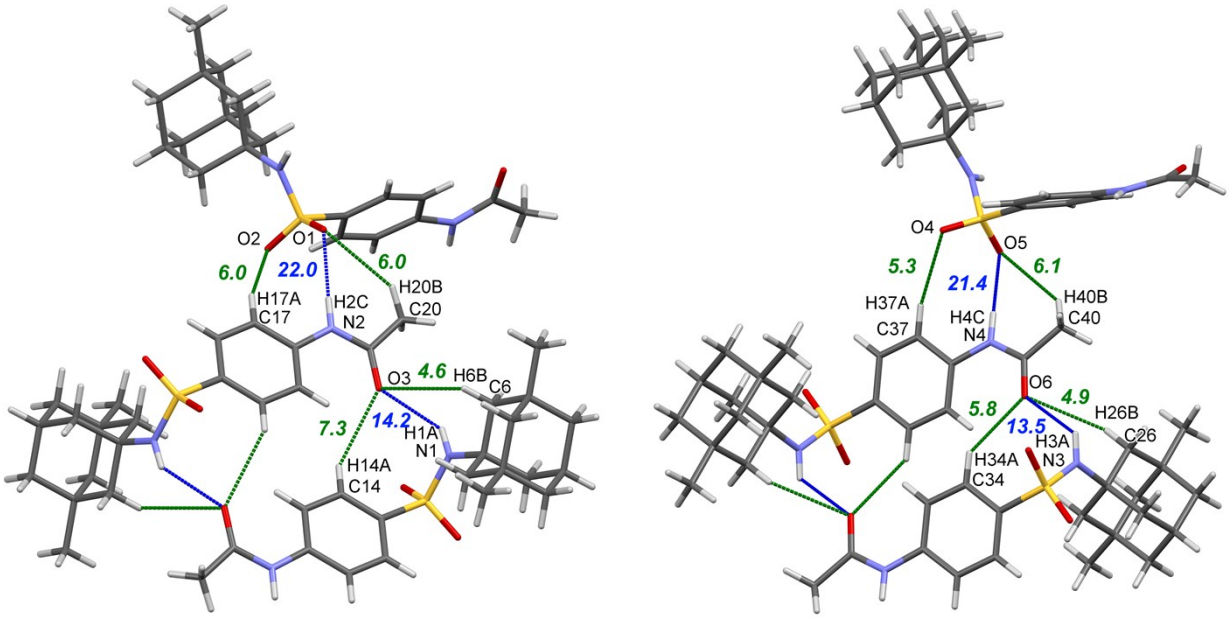

Fig. S4 Part of hydrogen bond network formed by molecules of compound **19** with different conformations. Numbers display the energies of notable hydrogen bonds (blue) and C-H···O contacts (green) estimated using eq.(S3).

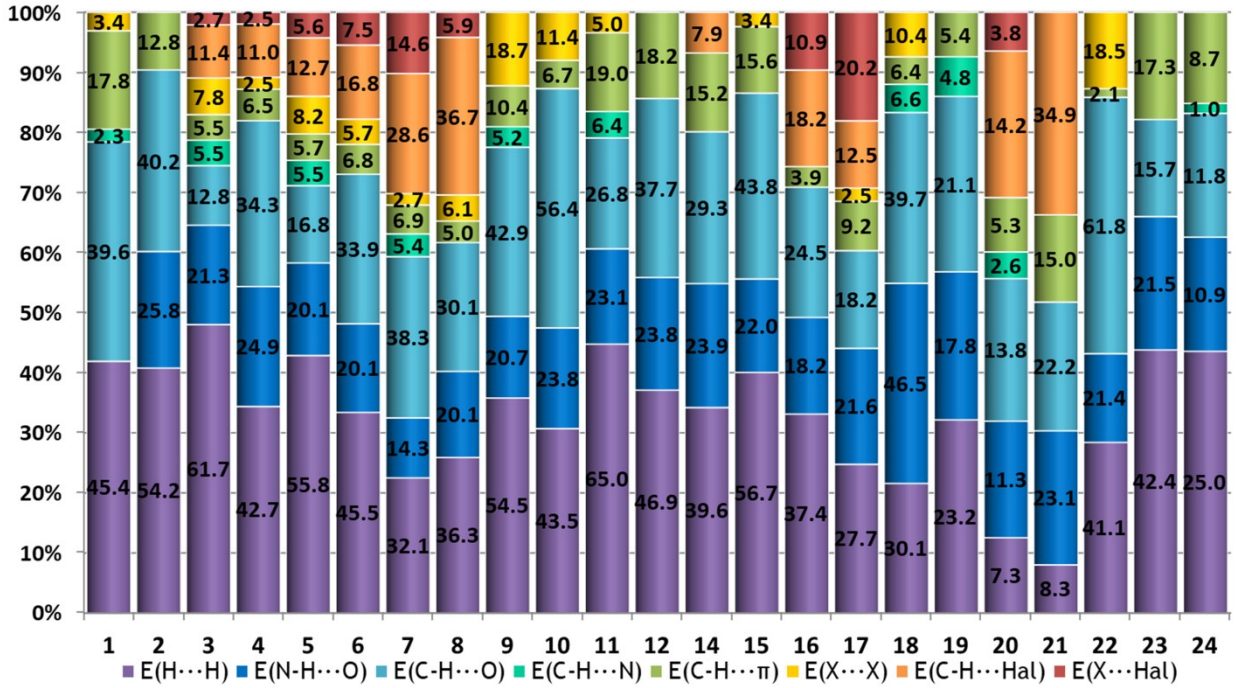

Fig. S5 Energies of intermolecular interactions between different atom types in the studied compounds calculated by QTAIMC plotted as percentages of lattice energy. The numbers display the total contribution of the interaction in kJ·mol^{-1}. X stands for C, N, and O atoms.

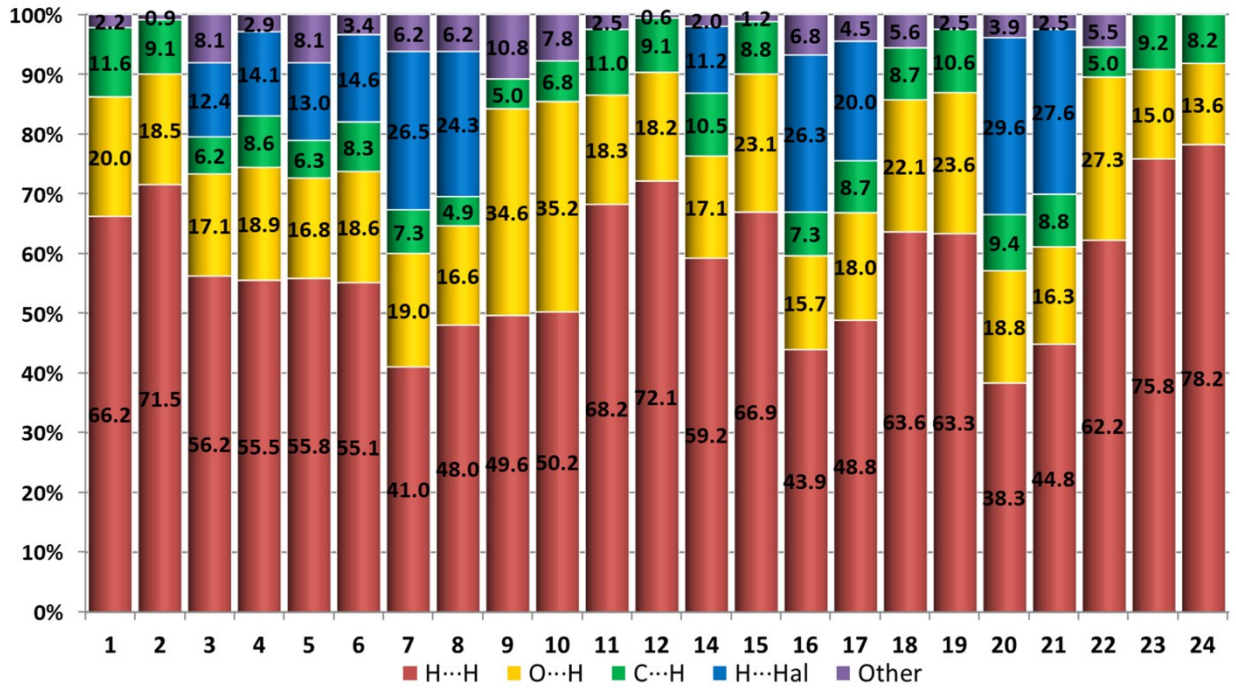

Fig. S6 Main contributions of intermolecular contacts between atoms of different types to the Hirshfeld surface for individual molecules within the crystal structures of the compounds under study.